Thermal conductivity control by oxygen defect concentration modification in reducible oxides: The case of $Pr_{0.1}Ce_{0.9}O_{2-\delta}$ thin films

Maria N. Luckyanova,[1] Di Chen,[2] Wen Ma,[3] Harry L. Tuller,[2] Gang Chen,[1,a)] and Bilge Yildiz[3,a)]
[1]*Department of Mechanical Engineering, Massachusetts Institute of Technology, Cambridge, Massachusetts 02139, USA*
[2]*Department of Materials Science and Engineering, Massachusetts Institute of Technology, Cambridge, Massachusetts 02139, USA*
[3]*Department of Nuclear Science and Engineering, Massachusetts Institute of Technology, Cambridge, Massachusetts 02139, USA*

(Received 23 December 2013; accepted 23 January 2014; published online 14 February 2014)

We demonstrate the impact on thermal conductivity of varying the concentration of oxygen vacancies and reduced cations in $Pr_{0.1}Ce_{0.9}O_{2-\delta}$ thin films prepared by pulsed laser deposition. The oxygen vacancy concentration is controlled by varying the oxygen partial pressure between 1×10^{-4} and 1 atm at 650 °C. Corresponding changes in the oxygen non-stoichiometry (δ) are monitored by detecting the lattice parameters of the films with high-resolution X-ray diffraction, while the thermal properties are characterized by time-domain thermoreflectance measurements. The films are shown to exhibit a variation in oxygen vacancy content, and in the Pr^{3+}/Pr^{4+} ratio, corresponding to changes in δ from 0.0027 to 0.0364, leading to a reduction in the thermal conductivity from $k = 6.62 \pm 0.61$ to 3.82 ± 0.51 W/m-K, respectively. These values agree well with those predicted by the Callaway and von Baeyer model for thermal conductivity in the presence of point imperfections. These results demonstrate the capability of controlling thermal conductivity via control of anion and cation defect concentrations in a given reducible oxide. [http://dx.doi.org/10.1063/1.4865768]

The thermal properties of oxides are of interest for a number of applications, including thermoelectrics,[1] thermal barrier coatings,[2,3] memristors,[4] and fuel cells.[5,6] Due to their strategic use as thermal barrier coatings in aerospace applications, a great deal of attention has already been focused on quantifying and understanding thermal transport in oxides. The existing work has, by and large, shown that oxygen vacancies play an important role in reducing the thermal conductivity of these materials.[7–11] Control of oxygen non-stoichiometry in oxides by thermal annealing is of interest for controlling the electrical and dielectric properties of varistors,[12] thermistors,[13] thermoelectrics,[14] and transparent conducting oxides,[15] just to name a few. Recently, there has been great interest in electric field induced resistance switching in memristors believed to be driven by the spatial redistribution of oxygen vacancies.[16] For this latter application, knowing the thin film thermal properties is believed to be important in modeling the behavior of these devices, but data on these properties remain scant.[17]

In this work, we investigate the dependence and tunability of the thermal conductivity of $Pr_{0.1}Ce_{0.9}O_{2-\delta}$ thin films as a model reducible oxide system. The non-stoichiometry of these films was previously investigated and characterized by the authors with the aid of chemical capacitance measurements.[18] This work shows the ability to vary the thermal conductivity of a material by control of oxygen non-stoichiometry and thus points to the possibility for *in situ* control of phonon transport via control of the oxygen vacancy concentration.

a)Authors to whom correspondence should be addressed. Electronic addresses: gchen2@mit.edu and byildiz@mit.edu

$Pr_{0.1}Ce_{0.9}O_{2-\delta}$ films were deposited onto (001) oriented single-crystal YSZ (8 mol. % Y_2O_3 stabilized) substrates ($10 \times 10 \times 0.5$ mm^3; MTI Corporation, Richmond, CA) by pulsed laser deposition (PLD, Neocera, Inc.) from oxide targets. The film grain size and surface roughness were determined by atomic force microscopy (Digital Instruments Nanoscope IIIa), and the film thickness was determined by surface profilometry (KLA-Tencor P-16+ stylus profiler). Further details related to the $Pr_{0.1}Ce_{0.9}O_{2-\delta}$ film preparation are discussed elsewhere.[19]

Following deposition, the samples were annealed at 650 °C and in oxygen partial pressures between 1×10^{-4} and 1 atm, controlled by mixing N_2 and O_2 with the aid of mass flow controllers and monitored by an *in situ* YSZ Nernst type oxygen sensor. The samples were quenched to room temperature after 12 h of annealing to freeze in the non-stoichiometry attained at elevated temperature.

The oxygen vacancy concentration is determined with high-resolution X-ray diffraction (HRXRD). The 2θ-ω scans (2θ is the angle between the incident and the diffracted X-ray beams; ω is the angle between the incident beam and the specimen surface) were carried out by a high resolution four-circle Bruker D8 Discover diffractometer, equipped with a Göbel mirror, Eulerian cradle, 3-bounce Ge 022 analyzer crystal and a scintillation counter, using Cu Kα1 radiation. The parallel beam condition, useful for eliminating various sources of error such as sample displacement error, flat specimen error, and sample transparency error, was satisfied by use of the combination of the Göbel mirror and the analyzer crystal.

In the strain-stress state analysis, diffraction lines of one or more *hkl* reflections are recorded at various tilts (ψ,ϕ).

From the measured peak positions, lattice strain is calculated from

$$\varepsilon^{hkl}_{\psi,\varphi} = (a^{hkl}_{\psi,\varphi} - a_0)/a_0, \quad (1)$$

where ψ is the angle of inclination of the specimen surface normal with respect to the diffraction vector, ϕ is the rotation of the specimen around the specimen surface normal, $a^{hkl}_{\psi,\varphi}$ is the lattice spacing measured for the $\{hkl\}$ reflection, and a_0 is the "stress-free" lattice parameter.

Since the $Pr_{0.1}Ce_{0.9}O_{2-\delta}$ (PCO) samples are epitaxial thin films with (001) orientation, the principal stresses in the film plane are equal, with a zero shear component ($\sigma_{11} = \sigma_{22} = \sigma_{//}, \sigma_{12} = 0$). Based on the crystallite group method (CGM),[20,21] the expression of lattice spacing vs. $\sin^2\psi$ for the [001] axis is

$$a^{001}_{\psi} = a_0[1 + (2s_{12} + (s_{11} - s_{12})\sin^2\psi)\sigma_{//}], \quad (2)$$

where s_{11} and s_{12} are the single-crystal compliances. Thus, the "stress-free" direction can be given by

$$\sin^2\psi = \frac{2s_{12}}{s_{12} - s_{11}}. \quad (3)$$

The lattice constants were measured at three inclination angles ψ, 0°, 25.24°, and 45° (Table I). The strain-free lattice parameters (a_0) were obtained by interpolating the a^{001}_{ψ} vs $\sin^2\psi$ with stress-free direction $\sin^2\psi^*$. Single-crystal elastic constants for CeO_2 were employed in this study to calculate the stress-free direction.[22]

In quantifying the oxygen vacancy concentration, the chemical expansion equation was used

$$\delta = \frac{\Delta a}{a_0 \alpha_{chem}}, \quad (4)$$

where δ is the oxygen non-stoichiometry factor in $Pr_{0.1}Ce_{0.9}O_{2-\delta}$, α_{chem} is the chemical expansion coefficient (0.08 for PCO),[23,24] and Δa is the change in the lattice constant, a_0. The fully reduced 10% PCO sample's lattice constant was used as the reference point ($\delta = 0.05$) in this equation.[25]

The thermal conductivity was measured using time-domain thermoreflectance (TDTR).[26–28] For the TDTR technique, a 100 nm optothermal transducer film of Al is deposited onto the samples using electron beam evaporation. A laser pulse impinges on the surface of the sample, exciting electrons at the surface that quickly thermalize, creating a heat pulse that propagates through the metal film, the sample, and the substrate. The reflectance of the surface decays with the temperature, and this changing reflectance is monitored with a time-delayed probe pulse. The resulting cooling curve is fit to a multi-dimensional, multi-layered solution to Fourier's heat equation. Details of the experimental system used herein have been described elsewhere.[29]

TABLE I. Values of (ψ,ϕ) corresponding to $\{hkl\}$ intensity poles of the [001] stereographic projection. 'x' indicates that there are no constraints.

Growth texture along the [001] direction			
{hkl}	200	311	440
Ψ (deg)	0	25.24	45
ϕ (deg)	x	45	0; 90

TABLE II. Anneal conditions, and the corresponding measured stress-free lattice constants and oxygen non-stoichiometries, δ, in $Pr_{0.1}Ce_{0.9}O_{2-\delta}$.

Sample	Condition	Lattice spacing, a_0 (Å)	Oxygen vacancy concentration, δ
T1 (PCO)	1 atm 650 °C	5.4107	0.0003
T2 (PCO)	0.1 atm 650 °C	5.4119	0.0031
T3 (PCO)	10^{-2} atm 650 °C	5.4190	0.0195
T4 (PCO)	10^{-4} atm 650 °C	5.4253	0.0341
T5 (PCO)	4% H_2 650 °C	5.4322	0.0500
T6 (PCO)	1 atm 400 °C	5.4110	0.0010
T7 (Ceria)	1 atm 400 °C	5.4130	0.0005

The measured stress-free lattice constants and oxygen non-stoichiometries in $Pr_{0.1}Ce_{0.9}O_{2-\delta}$ are listed in Table II and plotted in Figure 1. The standard error for the lattice constant as determined by XRD is 0.0005 Å. As the sample was annealed in ever more reducing conditions (T1–T5), the oxygen vacancy concentration increased accordingly, with the quenched-in values obtained for δ in samples T3 and T4 in excellent agreement with equilibrium values obtained previously by chemical capacitance.[18] At the higher pO_2s characteristic of T1 and T2, the frozen in values for δ were smaller than the equilibrium values due to partial reoxidation during cooling. The sample annealed in hydrogen (T5) was set as the reference oxygen vacancy concentration at $\delta = 0.05$ (meaning that all of the Pr^{4+} cations are reduced to Pr^{3+}).[18] The oxygen vacancy in the nominally undoped ceria film (T7) was estimated by assuming an acceptor impurity concentration of 100 ppm in the film, as is typical for these materials.[30]

The thermal conductivities of the six samples with different oxygen vacancy concentrations are shown in Figure 2. The results show that the thermal conductivity decreases with an increasing oxygen vacancy concentration. Callaway and von Baeyer presented a phenomenological model for capturing the effects of lattice point imperfections on the thermal conductivity.[8] The model accounts for both the effects from mass fluctuations and lattice distortions which cause strain field fluctuations. In the $Pr_{0.1}Ce_{0.9}O_{2-\delta}$ system, every additional

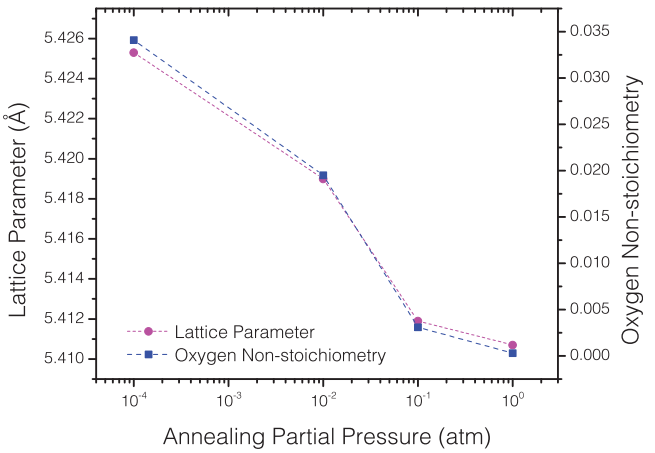

FIG. 1. $Pr_{0.1}Ce_{0.9}O_{2-\delta}$ lattice parameters determined from HRXRD and the resultant oxygen non-stoichiometries obtained from the chemical expansion equation as a function of oxygen partial pressures during annealing.

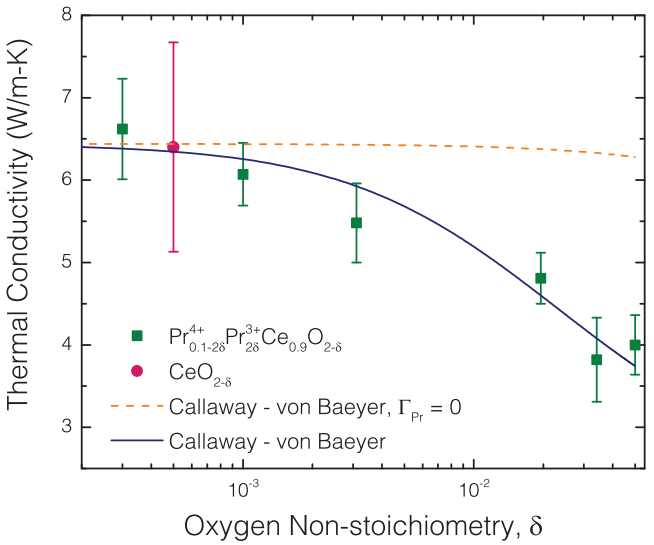

FIG. 2. Calculated and experimental thermal conductivity values of $Pr_{0.1}Ce_{0.9}O_{2-\delta}$ films with different oxygen non-stoichiometries, $\boldsymbol{\delta}$, and the thermal conductivity of a reference CeO_2 film with a nominal $\boldsymbol{\delta}$ of 0.005. Error bars represent the standard deviations in the measured results. Calculated results originate from the Callaway-von Baeyer model for thermal conductivity in the presence of point imperfections. The two sets of calculated results are for the modified thermal conductivity including the strain and mass fluctuations from only the oxygen vacancies (dashed line), and for the thermal conductivity including these effects as well as the effects of strain fluctuations resulting from the reduction of Pr^{4+} to Pr^{3+} (solid line).

oxygen vacancy results in the reduction of two Pr atoms, thus the complete stoichiometric formula is $Pr^{4+}_{0.1-2\delta}Pr^{3+}_{2\delta}Ce_{0.9}O_{2-\delta}$. Compared to the unreduced Pr^{4+}, the reduced Pr^{3+} increases in size by 14%.[31] The thermal conductivity k of the system in the presence of defects is given by

$$k = k_0 \frac{tan^{-1}(u)}{u}, \tag{5}$$

where k_0 is the thermal conductivity of the defect-free material and u is given by

$$u = \left(k_0 \frac{\pi^2 \Theta_D \Omega}{h v^2} \Gamma_{Pr_xCe_yO_z}\right)^{1/2}, \tag{6}$$

where Θ_D is the Debye temperature, Ω is the average atomic volume, and v is the average sound velocity. The mass and lattice defects are accounted for by the imperfection scaling parameter, $\Gamma_{Pr_xCe_yO_z}$, which represents the sum of the contributions from all the imperfections

$$\Gamma_{Pr_xCe_yO_z} = \frac{x}{x+y+z}\left(\frac{M_{Pr}}{\bar{M}}\right)^2 \Gamma_{Pr} + \frac{y}{x+y+z}\left(\frac{M_{Ce}}{\bar{M}}\right)^2 \Gamma_{Ce} + \frac{z}{x+y+z}\left(\frac{M_O}{\bar{M}}\right)^2 \Gamma_O, \tag{7}$$

where M_i is the average mass contributed by atom i, and $\bar{M}$ is the average mass of the compound. Since the Ce^{4+} ion remains unchanged during the reduction process, it's contribution to the imperfection parameter, Γ_{Ce}, is zero.

The contribution to the imperfection scaling parameter, Γ, from each element i is further subdivided into a mass component, $\Gamma_{i,m}$, and a lattice component, $\Gamma_{i,l}$

$$\Gamma_i = \Gamma_{i,m} + \Gamma_{i,l}. \tag{8}$$

In the case of Pr, the mass difference between the two charge states is negligible. Thus, the three contributions to the PCO imperfection scaling parameter result from the lattice fluctuations due to the oxygen vacancies and the change in the size of Pr, and the point mass fluctuations resulting from the oxygen vacancies.

The imperfection parameter due to mass fluctuations is given by

$$\Gamma_{i,m}(i,i') = c(1-c)\left(\frac{\Delta M}{M_{(i,i')}}\right)^2, \tag{9}$$

where ΔM is the mass difference between i and it's substitutive element i', $M_{(i,i')}$ is the weighted mass of element i, and c is the relative concentration of the impurity. The imperfection parameter due to strain from the lattice fluctuation is given simply by

$$\Gamma_{i,l}(i,i') = c(1-c)\varepsilon\left(\frac{\Delta\varsigma}{\varsigma_{(i,i')}}\right)^2, \tag{10}$$

where $\varsigma_{(i,i')}$ is the weighted average radius of element i, $\Delta\varsigma$ is the atomic radius difference between i and it's substitutive element i', and ε is a phenomenological adjustable parameter. This model relies on information about the Debye temperature and the speed of sound of PCO. Since this information is unreported, a reasonable estimate was to use the Debye temperature and speed of sound of undoped CeO_2 instead.[22,32] A least squares minimization algorithm was used to determine that $\varepsilon = 20$ yields the curve of best fit to the data, a value that falls within the expected range. The results of this model are shown in Figure 2 and match well to the experimental results.

Figure 2 shows both the results of the modeling including just the effects of the oxygen vacancies and effects both from the oxygen vacancies and Pr reduction from 4+ to 3+. The results demonstrate that the effects of the lattice distortions caused by the reduction of the Pr are much greater than those of the mass effects from the oxygen vacancies. This can be understood both by the very small relative contribution of the oxygen to the overall mass of the compound, the fact that each oxygen vacancy actually impacts the size of two Pr atoms, as well as the larger lattice distortions induced by the large Pr^{3+} cation compared to the lattice distortions due to an oxygen vacancy.[33,34]

In conclusion, we have demonstrated a strong impact on the thermal conductivity of reducing an oxide system, $Pr_{0.1}Ce_{0.9}O_{2-\delta}$, ultimately creating point defects of oxygen vacancies and reduced Pr cations. The thermal conductivity varies by nearly 50%, a result that matches well with that predicted by the Callaway–von Baeyer model for thermal conductivity in the presence of point defects. Because oxygen non-stoichiometry can be controlled in a reversible manner in such films, this points to the possibility of controlling thermal conductivity via *in situ* defect control.

This work was supported primarily by the MIT MRSEC through the MRSEC Program of the National Science

Foundation under Award No. DMR-0819762. This work made use of the MIT MRSEC Shared Experimental Facilities supported by the National Science Foundation under Award No. DMR-0819762.

[1]I. Terasaki, Y. Sasago, and K. Uchinokura, Phys. Rev. B **56**, R12685 (1997).
[2]N. P. Padture, M. Gell, and E. H. Jordan, Science **296**, 280 (2002).
[3]D. Clarke and S. Phillpot, Mater. Today **8**, 22 (2005).
[4]J. J. Yang, D. B. Strukov, and D. R. Stewart, Nat. Nanotechnol. **8**, 13 (2013).
[5]A. Faghri and Z. Guo, Int. J. Heat Mass Transf. **48**, 3891 (2005).
[6]M. Khandelwal and M. M. Mench, J. Power Sources **161**, 1106 (2006).
[7]P. Klemens, Phys. Rev. **119**, 507 (1960).
[8]J. Callaway and H. von Baeyer, Phys. Rev. **120**, 1149 (1960).
[9]C. Walker and R. Pohl, Phys. Rev. **131**, 1433 (1963).
[10]P. G. Klemens, Phys. Condens. Matter **263–264**, 102 (1999).
[11]P. G. Klemens and M. Gell, Mater. Sci. Eng. A **245**, 143 (1998).
[12]R. van de Krol and H. Tuller, Solid State Ionics **150**, 167 (2002).
[13]D. C. Hill and H. L. Tuller, in *Ceramic Materials and Electronics*, edited by R. C. Buchanan and M. Dekker, 2nd ed. (New York, 1991), pp. 249–347.
[14]J. He, Y. Liu, and R. Funahashi, J. Mater. Res. **26**, 1762 (2011).
[15]A. Janotti and C. G. Van de Walle, Rep. Prog. Phys. **72**, 126501 (2009).
[16]D. B. Strukov, G. S. Snider, D. R. Stewart, and R. S. Williams, Nature **453**, 80 (2008).
[17]P. G. Klemens, Int. J. Thermophys. **22**, 265 (2001).
[18]D. Chen, S. R. Bishop, and H. L. Tuller, Adv. Funct. Mater. **23**, 2168 (2013).
[19]D. Chen, S. R. Bishop, and H. L. Tuller, J. Electroceram. **28**, 62 (2012).
[20]G. Abadias, Surf. Coat. Technol. **202**, 2223 (2008).
[21]U. Welzel, J. Ligot, P. Lamparter, A. C. Vermeulen, and E. J. Mittemeijer, J. Appl. Crystallogr. **38**, 1 (2005).
[22]V. Kanchana, G. Vaitheeswaran, A. Svane, and A. Delin, J. Phys. Condens. Matter **18**, 9615 (2006).
[23]Y. Kuru, D. Marrocchelli, S. R. Bishop, D. Chen, B. Yildiz, and H. L. Tuller, J. Electrochem. Soc. **159**, F799 (2012).
[24]Y. Kuru, S. R. Bishop, J. J. Kim, B. Yildiz, and H. L. Tuller, Solid State Ionics **193**, 1 (2011).
[25]Y. Wang, T. Mori, J.-G. Li, and T. Ikegami, J. Am. Ceram. Soc. **85**, 3105 (2004).
[26]D. G. Cahill, Rev. Sci. Instrum. **75**, 5119 (2004).
[27]D. G. Cahill, K. Goodson, and A. Majumdar, J. Heat Transfer **124**, 223 (2002).
[28]W. S. Capinski and H. J. Maris, Rev. Sci. Instrum. **67**, 2720 (1996).
[29]A. J. Schmidt, X. Chen, and G. Chen, Rev. Sci. Instrum. **79**, 114902 (2008).
[30]S. J. Litzelman and H. L. Tuller, Solid State Ionics **180**, 1190 (2009).
[31]R. D. Shannon, Acta Crystallogr. A **32**, 751 (1976).
[32]T. Hisashige, Y. Yamamura, and T. Tsuji, J. Alloys Compd. **408–412**, 1153 (2006).
[33]D. Marrocchelli, S. R. Bishop, H. L. Tuller, G. W. Watson, and B. Yildiz, Phys. Chem. Chem. Phys. **14**, 12070 (2012).
[34]D. Marrocchelli, S. R. Bishop, H. L. Tuller, and B. Yildiz, Adv. Funct. Mater. **22**, 1958 (2012).